JACS
JOURNAL OF THE AMERICAN CHEMICAL SOCIETY
Communication
pubs.acs.org/JACS

Design and Synthesis of Metal Sulfide Catalysts Supported on Zeolite Nanofiber Bundles with Unprecedented Hydrodesulfurization Activities

Tiandi Tang,*[,†] Lei Zhang,[†] Wenqian Fu,[†] Yuli Ma,[†] Jin Xu,[†] Jun Jiang,[†] Guoyong Fang,[†] and Feng-Shou Xiao*[,‡]

[†]College of Chemical and Materials Engineering, Wenzhou University, Wenzhou 325035, P. R. China
[‡]Department of Chemistry, Zhejiang University, Hangzhou 310028, P. R. China

Supporting Information

ABSTRACT: Developing highly active hydrodesulfurization (HDS) catalysts is of great importance for producing ultraclean fuel. Herein we report on crystalline mordenite nanofibers (NB-MOR) with a bundle structure containing parallel mesopore channels. After the introduction of cobalt and molybdenum (CoMo) species into the mesopores and micropores of NB-MOR, the NB-MOR-supported CoMo catalyst (CoMo/NB-MOR) exhibited an unprecedented high activity (99.1%) as well as very good catalyst life in the HDS of 4,6-dimethyldibenzothiophene compared with a conventional γ-alumina-supported CoMo catalyst (61.5%). The spillover hydrogen formed in the micropores migrates onto nearby active CoMo sites in the mesopores, which could be responsible for the great enhancement of the HDS activity.

Increasingly stringent environmental legislation is pressuring manufacturers to reduce the sulfur content in gasoline and diesel fuel to a level of 10 ppm and lower.[1] To reach this low sulfur level, even highly refractory sulfur compounds in the fuel, such as 4,6-dimethyldibenzothiophene (4,6-DMDBT), must be almost completely removed.[2] Generally, conventional hydrodesulfurization (HDS) catalysts, γ-alumina-supported metal sulfides (CoMo/γ-Al_2O_3 or NiMo/γ-Al_2O_3), have difficulty in fully removing 4,6-DMDBT because of steric hindrance by the methyl groups adjacent to the sulfur atom.[3] One solution to this problem is to increase the hydrogenating ability by replacing the metal sulfides by noble metals.[4] However, the relatively short catalyst life and high cost of these noble metals strongly limit their applications.[5]

It has been reported that hydrogen spillover can greatly enhance the hydrogenating ability;[6] thus, an improvement of the hydrogen spillover ability of conventional HDS catalysts would facilitate very high HDS activities.[7] Thanks to recent successful syntheses on mesoporous zeolites,[8] it should be possible to design catalytic active sites in micropores and mesopores of mesoporous zeolites that have hydrogen spillover ability and hydrogenating ability, respectively.

Herein we first report a facile method to synthesize nanofiber bundles of the zeolite mordenite (NB-MOR). The resulting material has parallel mesopore channels in the nanofiber bundles of the microporous MOR zeolite. In addition, after the introduction of cobalt and molybdenum (CoMo) species in the mesopores and micropores followed by sulfidation, the NB-MOR-supported CoMo catalyst (CoMo/NB-MOR) exhibited an unprecedented high activity in the HDS of 4,6-DMDBT compared with conventional CoMo(NiMo)/γ-Al_2O_3 catalysts. This feature may be attributed to the migration of spillover hydrogen formed in the micropores onto nearby active CoMo sites in the mesopores, which significantly enhances the hydrogenating ability of the catalyst. This catalyst design concept provides a new strategy for the rational preparation of multifunctional highly active catalysts.

Despite the recent successful syntheses of nanosized zeolite materials such as nanosheets and nanoparticles using mesoscale organic templates,[9] it is difficult to obtain zeolite nanofibers by a similar route. In this work, we synthesized a random cationic copolymer containing quaternary ammonium groups and used it as a template for the synthesis of mordenite zeolite nanofibers, which can be assembled to a bundle structure [section S1 in the Supporting Information (SI)].

Figure 1 shows the X-ray diffraction (XRD) pattern, N_2 sorption isotherm, and scanning electron microscopy (SEM) and transmission electron microscopy (TEM) images of NB-MOR. The XRD pattern shows well-resolved peaks in the range 4−40°, which correspond to the MOR zeolite structure (Figure 1a). The N_2 sorption isotherm of NB-MOR exhibits a hysteresis loop at a relative pressure of 0.45−0.96, which is typically assigned to the presence of mesostructure (Figure 1b). Correspondingly, the mesopore size distribution of the NB-MOR is mainly centered at 13 nm (Figure 1b inset). Sample textural parameters are presented in Table S2 in the SI. The SEM images (Figure 1c,d) reveal that NB-MOR has a particle size of 3 μm × 5 μm. The NB-MOR particles consist of parallel zeolite nanofibers with diameters of 10−30 nm that are aggregated into bundles (Figure 1d−f). In this manner, parallel mesoporous channels are formed in the aggregated bundles (Figure S2 in the SI). Furthermore, the fast Fourier transform (FFT) of the NB-MOR TEM image (Figure 1f inset) shows that the *b* axis of MOR (010 face, pore size of 3.4 Å × 4.8 Å) is perpendicular to the mesopore direction. This micropore−mesopore structural feature could be beneficial for mass transfer of small molecules such as H_2 from the micropores to the mesopores.

Received: May 1, 2013
Published: July 19, 2013

dx.doi.org/10.1021/ja4043388 | J. Am. Chem. Soc. 2013, 135, 11437−11440

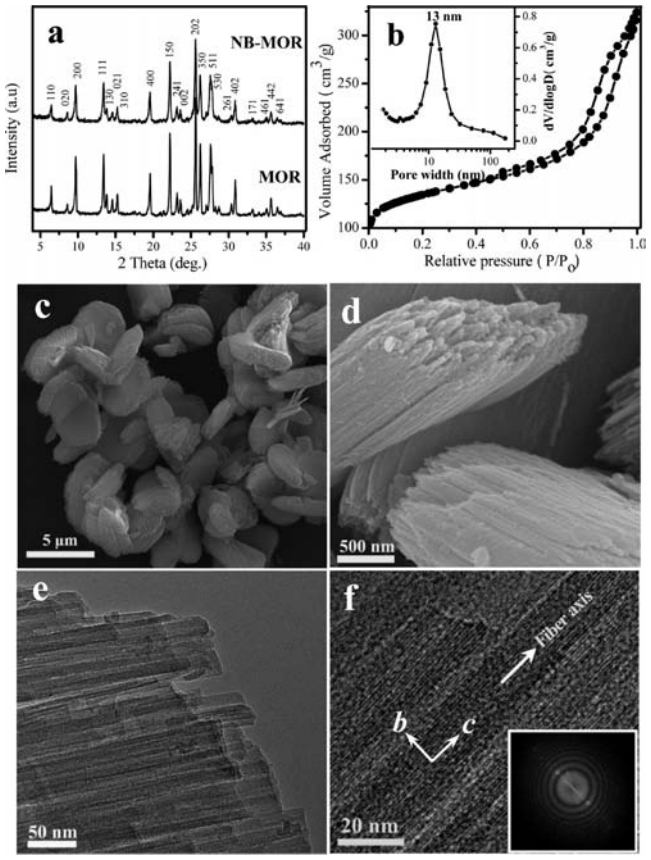

Figure 1. (a) XRD patterns, (b) N_2 adsorption isotherm, (c) low-resolution SEM image, (d) high-resolution SEM image, (e) low-resolution TEM image and (f) high-resolution TEM image and (inset) FFT of the NB-MOR sample.

In catalyst preparation, the aim was to disperse the active metal species not only in the mesoporous channels but also in the micropores of NB-MOR. To introduce the active metal species into the support micropores, the pH of the impregnation solution was adjusted to ~10.0. In this case, most of the $Mo_7O_{24}^{6-}$ was converted to small MoO_4^{2-} species,[10] which could easily penetrate into the micropores of NB-MOR. After sulfidation by a mixture of H_2 and H_2S (400 °C, 10 vol % H_2S), the $CoMoS_2$ phases (marked by white arrows) were uniformly located in the parallel mesopore channels of NB-MOR (Figure 2a,b). Moreover, very small metal sulfide clusters may be formed in the micropores of the zeolite. This suggestion was confirmed by additional TEM images and energy-dispersive X-ray spectroscopy (EDS) analysis of a thin-sectioned sulfided microporous Mo/MOR catalyst sample (Figures S3–S6). The TEM images of a selected zone of the microporous Mo/MOR catalyst sample (Figures S3 and S4) show that the catalyst contained only micropores and that no larger MoS_2 nanoparticles were present. However, the EDS elemental mapping of the selected zone confirmed the presence of Mo and S (Figure S5); the atomic Mo/S ratio was ~0.88 (Table S3). This suggested that only very small metal sulfide clusters (MoS_x, $1 < x < 2$) were highly dispersed in the micropores of the MOR zeolite. Interestingly, after destruction of the ordered micropores by the strong electron beam, larger nanoparticles (1–2 nm) were observed (Figure S6). The large nanoparticles are attributed to aggregation of the very small metal sulfide clusters. These results also indicate that the micropores of the Mo/MOR catalyst sample contained very small metal sulfide clusters. It is worth noting that results published previously showed that very small metal sulfide clusters such as Ni–Mo–S and MoS_x could be dispersed inside the micropores of zeolite Y and ZSM-5.[11] The authors also suggested that the MoS_x or Ni–Mo–S clusters inside the zeolite micropores were more active in toluene hydrogenation and HDS of dibenzothiophene than MoS_2 slabs.[11b,c] In addition, the argon sorption results showed that the micropore size distribution and micropore volume decreased with increased metal loading in NB-MOR (Figure S7). This phenomenon might be related to the existence of the very small metal sulfide clusters in the micropores of NB-MOR.

Figure 3 shows catalytic data for HDS of 4,6-DMDBT over activated CoMo/NB-MOR and CoMo/γ-Al_2O_3 catalysts. The reaction network of 4,6-DMDBT HDS is shown in Figure S8. Compared with CoMo/γ-Al_2O_3 (61.5%), the CoMo/NB-MOR catalyst exhibited very high 4,6-DMDBT conversion (99.1%) (Figure 3a). Correspondingly, the lowest remaining sulfur content in the reaction products over CoMo/NB-MOR was 12 ppm, while that over the CoMo/γ-Al_2O_3 catalyst was 331 ppm (Figure 3b). These results indicate that the CoMo/NB-MOR catalyst shows an unprecedented high HDS activity. Very importantly, the CoMo/NB-MOR catalyst shows a long catalyst life. There was no activity loss for the CoMo/NB-MOR catalyst in the HDS of 4,6-DMDBT (Figure 3c). The good catalyst life of the CoMo/NB-MOR catalyst is one of the key features in applications of industrial catalysts. Additionally, the yield of

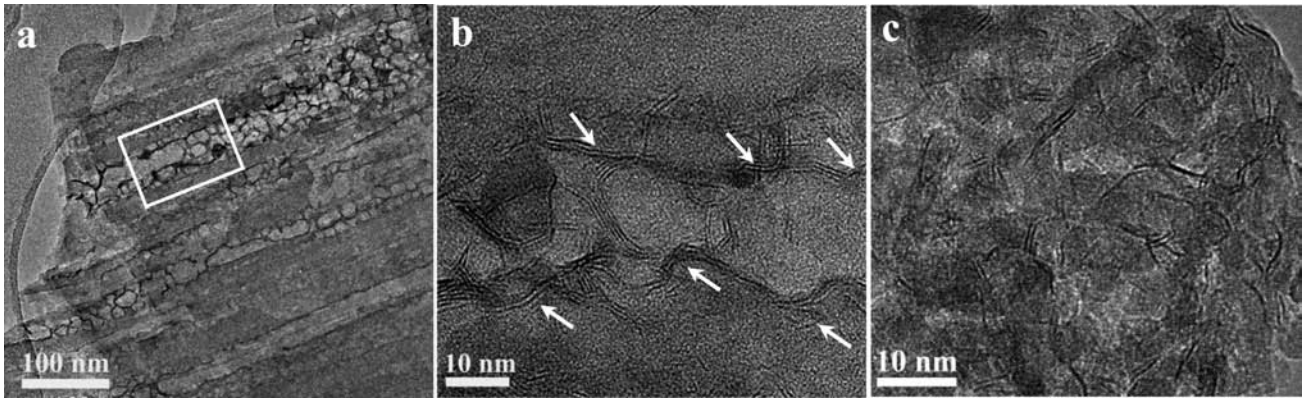

Figure 2. (a) Low-resolution TEM image of the sulfided CoMo/NB-MOR catalyst. (b) High-resolution TEM image of the selected area marked by the white square in (a). (c) High-resolution TEM image of the sulfided CoMo/γ-Al_2O_3 catalyst.

dx.doi.org/10.1021/ja4043388 | J. Am. Chem. Soc. 2013, 135, 11437–11440

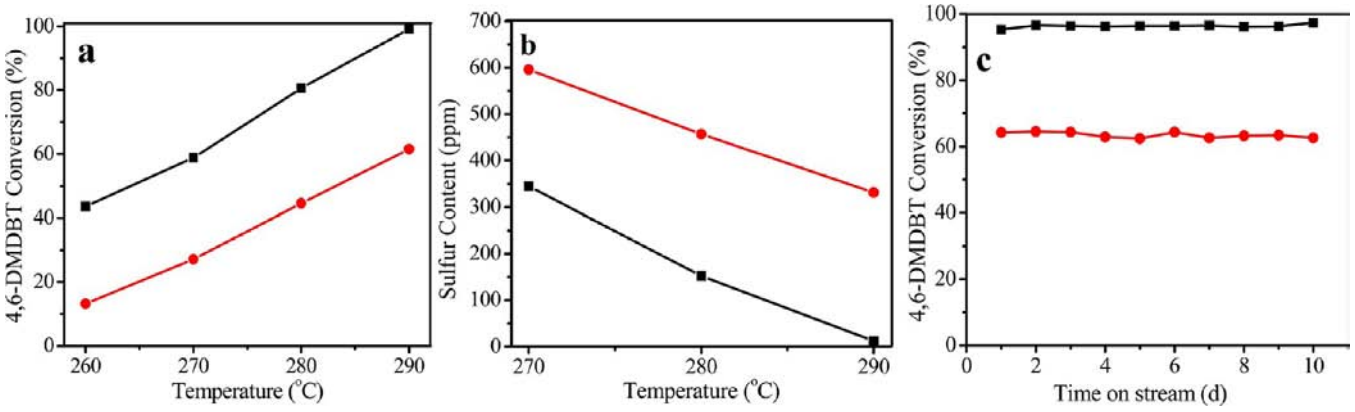

Figure 3. Activities of the catalysts. (a) 4,6-DMDBT conversion and (b) the remaining sulfur content in the reaction products at different temperatures over (black ■) CoMo/NB-MOR and (red ●) CoMo/γ-Al_2O_3 catalysts. (c) Reaction time dependence of 4,6-DMDBT conversion over (black ■) CoMo/NB-MOR and (red ●) CoMo/γ-Al_2O_3 catalysts. Reaction conditions: total pressure, 5.0 MPa; temperature, 290 °C; feed stock, 0.5 wt % 4,6-DMDBT in decalin; feed solution weight hourly space velocity, 14.6 h^{-1}; H_2/oil = 700. The two catalysts had the same metal loading; the Co/Mo molar ratio was 1:2, and the Mo loading was 10.7 wt %.

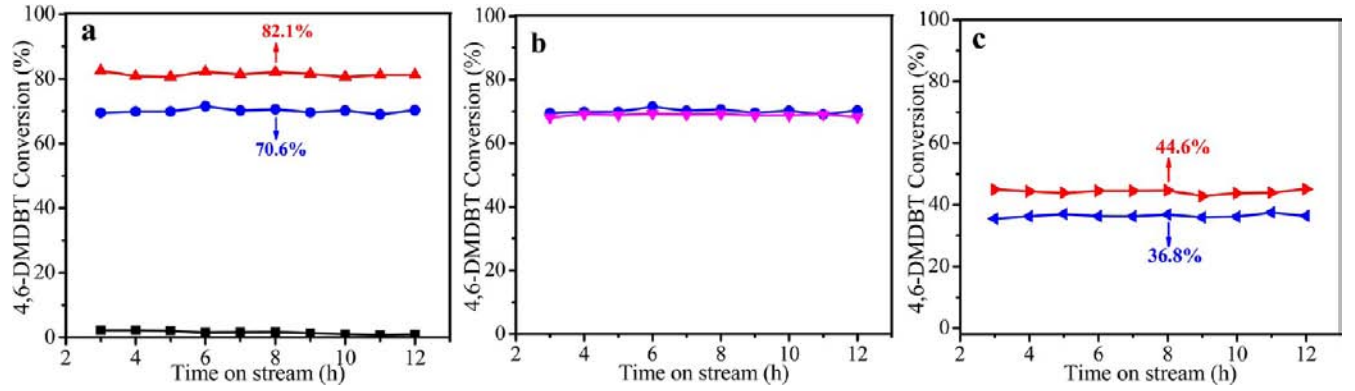

Figure 4. Reaction time dependences of 4,6-DMDBT conversion over a series of catalysts in hydrogen spillover experiments: (a) (black ■) 0.2 g of CoMo/MOR (2.7 wt % Mo), (blue ●) 0.3 g of CoMo/NB-MOR (12.5 wt % Mo), and (red ▲) 0.3 g of CoMo/NB-MOR (10.7 wt % Mo) mixed with 0.2 g of CoMo/MOR (2.7 wt % Mo); (b) (blue ●) 0.3 g of CoMo/NB-MOR (12.5 wt % Mo) and (purple ▼) 0.3 g of CoMo/NB-MOR (12.5 wt % Mo) mixed with 0.2 g of MOR; (c) (blue left-pointing triangles) 0.3 g of CoMo/γ-Al_2O_3 (12.5 wt % Mo) and (red right-pointing triangles) 0.3 g of CoMo/γ-Al_2O_3 (10.7 wt % Mo) mixed with 0.2 g of CoMo/MOR (2.7 wt % Mo). For all of the catalysts, the Co/Mo molar ratio was 1:2.

hydrocracking products (C_5−C_9) over the CoMo/NB-MOR catalyst (0.10%) was very low (Table S4), which is also an important factor for industrial applications of HDS catalysts.

It is worth mentioning that in addition to the CoMo/NB-MOR catalyst, the NiMo/NB-MOR catalyst exhibited excellent HDS activity (Figure S9). Moreover, we also tested the HDS activity of CoMo/NB-MOR for treatment of industrial diesel with a sulfur content of 5240 ppm. After 10 h of reaction, the remaining sulfur content in the product was below 20 ppm over the CoMo/NB-MOR catalyst, which is much lower than the value of ∼500 ppm obtained over the CoMo/γ-Al_2O_3 catalyst (Figure S10). These results show the potential importance of industrial applications of the CoMo/NB-MOR catalyst in the future.

Because of the large size of the 4,6-DMDBT molecule, HDS occurs mainly in the mesopores rather than in the micropores over the CoMo/NB-MOR catalyst. Notably, although γ-Al_2O_3 has a larger mesopore surface area (288 m^2/g) than NB-MOR (182 m^2/g), the CoMo/NB-MOR catalyst exhibits much higher activity than the CoMo/γ-Al_2O_3 catalyst at the same metal loading. This phenomenon is attributed to the difference in the microporosities of the NB-MOR and γ-Al_2O_3 supports. NB-MOR has a mesopore volume of 0.37 cm^3/g as well as a micropore volume of 0.13 cm^3/g, while γ-Al_2O_3 has only a mesopore volume of 0.45 cm^3/g (Table S2). It is possible that the small molybdenum sulfide clusters in the micropores of the NB-MOR support create a large amount of spillover hydrogen, which then migrates onto nearby active CoMo sites in the mesopores, enhancing the hydrogenating ability of the CoMo/NB-MOR catalyst. This suggestion was strongly supported by catalytic tests over a mesopore-free MOR-supported CoMo catalyst (CoMo/MOR) and mechanical mixtures of CoMo/NB-MOR or CoMo/γ-Al_2O_3 with CoMo/MOR (Figure 4). When the mesopore-free MOR support was used, the CoMo/MOR catalyst showed very low conversion (1.7%) because the HDS of the bulky 4,6-DMDBT molecule occurred only on the external surface of the CoMo/MOR catalyst (Figure 4a). However, when the CoMo/NB-MOR catalyst was mechanically mixed with CoMo/MOR, the conversion reached 82.1%. In contrast, CoMo/NB-MOR itself showed a conversion of 70.6% (Figure 4a). Interestingly, when pure MOR zeolite was added to CoMo/NB-MOR, the catalyst activity was close to that of CoMo/NB-MOR itself (Figure 4b). These results indicate that the very small metal sulfide clusters in the micropores play an important role in enhancing the HDS activity of the CoMo/NB-MOR catalyst. As expected, the 4,6-DMDBT conversion was also improved when

dx.doi.org/10.1021/ja4043388 | J. Am. Chem. Soc. 2013, 135, 11437−11440

CoMo/γ-Al_2O_3 was mixed with the CoMo/MOR catalyst, increasing from 36.8% to 44.6% (Figure 4c). Furthermore, the selectivities for the hydrogenation products confirmed that the hydrogenating ability of both the CoMo/NB-MOR and CoMo/γ-Al_2O_3 catalysts was remarkably increased by mixing with CoMo/MOR (Table S5). Moreover, temperature-programmed desorption of ammonia (NH_3-TPD) curves showed that the acidity of the CoMo/NB-MOR catalyst was higher than that of the CoMo/γ-Al_2O_3 catalyst (Figure S11). Thus, the CoMo/NB-MOR catalyst exhibits higher selectivities for toluene and methylcyclohexane than the CoMo/γ-Al_2O_3 catalyst (Table S5) due to the cracking of 3,3′-dimethylcyclohexylbenzene.

In summary, we have demonstrated a facile method for synthesizing novel zeolite nanofiber bundles containing parallel mesopore channels. More importantly, CoMo and NiMo catalysts supported on these nanofiber bundles showed an unprecedented high activity and excellent catalyst life in the HDS of 4,6-DMDBT and industrial diesel compared with a conventional γ-alumina-supported CoMo catalyst. These features should be important in the future for the design and preparation of multifunctional high activity catalysts for HDS, selective cracking, and hydrocracking.

■ ASSOCIATED CONTENT

Supporting Information

Experimental details, catalyst tests, characterization, and HDS product selectivity. This material is available free of charge via the Internet at http://pubs.acs.org.

■ AUTHOR INFORMATION

Corresponding Author

tangtiandi@wzu.edu.cn; fsxiao@zju.edu.cn

Notes

The authors declare no competing financial interest.

■ ACKNOWLEDGMENTS

This work was supported by the National Natural Science Foundation of China (U1162115 and 21076163) and the Natural Science Foundation of Zhejiang Province of China (Y4090084). The authors thank the anonymous reviewers for the invaluable advice.

■ REFERENCES

(1) Yang, R. T.; Hernández-Maldonado, A. J.; Yang, F. H. *Science* **2003**, *301*, 79.

(2) (a) Song, C.; Ma, X. *Appl. Catal., B* **2003**, *41*, 207. (b) Li, X.; Wang, A.; Egorova, M.; Prins, R. *J. Catal.* **2007**, *250*, 283. (c) Sun, Y.; Prins, R. *Angew. Chem., Int. Ed.* **2008**, *47*, 8478. (d) Stanislaus, A.; Marafi, A.; Rana, M. S. *Catal. Today* **2010**, *153*, 1. (e) Fan, Y.; Xiao, H.; Shi, G.; Liu, H.; Qian, Y.; Wang, T.; Gong, G.; Bao, X. *J. Catal.* **2011**, *279*, 27.

(3) (a) Houalla, M.; Nag, N. K.; Sapre, A. V.; Broderick, D. H.; Gates, B. C. *AIChE J.* **1978**, *24*, 1015. (b) Corma, A. *Chem. Rev.* **1997**, *97*, 2373. (c) Gates, B. C.; Topsøe, H. *Polyhedron* **1997**, *16*, 3213. (d) Meille, V.; Schulz, E.; Lemaire, M.; Vrinat, M. *J. Catal.* **1997**, *170*, 29. (e) Whitehurst, D. D.; Isoda, T.; Mochida, I. *Adv. Catal.* **1998**, *42*, 345. (f) Bataille, F.; Lemberton, J.; Michaud, P.; Pérot, G.; Vrinat, M.; Lemaire, M.; Schulz, E.; Breysse, M.; Kasztelan, S. *J. Catal.* **2000**, *191*, 409. (g) Bej, S. K.; Maity, S. K.; Turaga, U. T. *Energy Fuels* **2004**, *18*, 1227. (h) Shu, Y.; Lee, Y. K.; Oyama, S. T. *J. Catal.* **2005**, *236*, 112. (i) Fujikawa, T.; Kimura, H.; Kiriyama, K.; Hagiwara, K. *Catal. Today* **2006**, *111*, 188. (j) Kibsgaard, J.; Lauritsen, J. V.; Lægsgaard, E.; Clausen, B. S.; Topsøe, H.; Besenbacher, F. *J. Am. Chem. Soc.* **2006**, *128*, 13950. (k) Lauritsen, J. V.; Kibsgaard, J.; Helveg, S.; Topsøe, H.; Clausen, B. S.; Lægsgaard, E.; Besenbacher, F. *Nat. Nanotechnol.* **2007**, *2*, 53. (l) Wang, A.; Qin, M.; Guan, J.; Wang, L.; Guo, H.; Li, X.; Wang, Y.; Prins, R.; Hu, Y. *Angew. Chem., Int. Ed.* **2008**, *47*, 6052. (m) Oyama, S. T.; Lee, Y. K. *J. Catal.* **2008**, *258*, 393. (n) Hansen, L. P.; Ramasse, Q. M.; Kisielowski, C.; Brorson, M.; Johnson, E.; Topsøe, H.; Helveg, S. *Angew. Chem., Int. Ed.* **2011**, *50*, 10153.

(4) (a) Topsøe, N. Y.; Tuxen, A.; Hinnemann, B.; Lauritsen, J. V.; Knudsen, K. G.; Besenbacher, F.; Topsøe, H. *J. Catal.* **2011**, *279*, 337. (b) Cooper, B. H.; Donnis, B. B. L. *Appl. Catal., A* **1996**, *137*, 203. (c) Niquille-Röthlisberger, A.; Prins, R. *J. Catal.* **2006**, *242*, 207. (d) Tang, T.; Yin, C.; Wang, L.; Ji, Y.; Xiao, F.-S. *J. Catal.* **2008**, *257*, 125. (e) Sun, Y.; Wang, H.; Prins, R. *Catal. Today* **2010**, *150*, 213. (f) Fu, W.; Zhang, L.; Tang, T.; Ke, Q.; Wang, S.; Hu, J.; Fang, G.; Li, J.; Xiao, F.-S. *J. Am. Chem. Soc.* **2011**, *133*, 15346.

(5) (a) Stanislaus, A.; Cooper, B. H. *Catal. Rev.: Sci. Eng.* **1994**, *36*, 75. (b) Yoshimura, Y.; Yasuda, H.; Sato, T.; Kijima, N.; Kameoka, T. *Appl. Catal., A* **2001**, *207*, 303. (c) Zhang, L.; Fu, W.; Ke, Q.; Zhang, S.; Jin, H.; Hu, J.; Wang, S.; Tang, T. *Appl. Catal., A* **2012**, *433*−*434*, 251. (d) Shantz, D. F.; Auf der Günne, J. S.; Koller, K.; Lobo, R. F. *J. Am. Chem. Soc.* **2000**, *122*, 6659. (e) Nash, M. J.; Shough, A. M.; Fickel, D. W.; Doren, D. J.; Lobo, R. F. *J. Am. Chem. Soc.* **2008**, *130*, 2460.

(6) (a) Sermon, P. A.; Bond, G. C. *Catal. Rev.: Sci. Eng.* **1974**, *8*, 211. (b) Lin, S. D.; Vannice, M. A. *J. Catal.* **1993**, *143*, 539. (c) Lin, S. D.; Vannice, M. A. *J. Catal.* **1993**, *143*, 554. (d) Lin, S. D.; Vannice, M. A. *J. Catal.* **1993**, *143*, 563. (e) Simon, L.; van Ommen, J. G.; Jentys, A.; Lercher, J. A. *J. Phys. Chem. B* **2000**, *104*, 11644. (f) Simon, L.; van Ommen, J. G.; Jentys, A.; Lercher, J. A. *J. Catal.* **2001**, *203*, 434. (g) Prins, R. *Chem. Rev.* **2012**, *112*, 2714.

(7) (a) de León, S. G.; Grange, P.; Delmon, B. *Stud. Surf. Sci. Catal.* **1993**, *77*, 345. (b) Pille, R. C.; Yu, C.; Froment, G. F. *J. Mol. Catal.* **1994**, *94*, 369. (c) Delmon, B.; Froment, G. F. *Catal. Rev.: Sci. Eng.* **1996**, *38*, 69. (d) Barton, D. G.; Soled, S. L.; Meitzner, G. D.; Fuentes, G. A.; Iglesia, E. *J. Catal.* **1999**, *181*, 57. (e) Ojeda, J.; Escalona, N.; Baeza, P.; Escudey, M.; Gil-Llambías, F. J. *Chem. Commun.* **2003**, 1608.

(8) (a) Davis, M. E. *Nature* **2002**, *417*, 813. (b) Xiao, F.-S.; Wang, L.; Yin, C.; Lin, K.; Di, Y.; Li, J.; Xu, R.; Su, D.; Schlögl, R.; Yokoi, T. *Angew. Chem., Int. Ed.* **2006**, *45*, 3090. (c) Choi, M.; Cho, H. S.; Srivastava, R.; Venkatesan, C.; Choi, D. H.; Ryoo, R. *Nat. Mater.* **2006**, *5*, 718. (d) Wang, H.; Pinnavaia, T. J. *Angew. Chem., Int. Ed.* **2006**, *45*, 7603. (e) Na, K.; Jo, C.; Kim, J.; Cho, K.; Jung, J.; Seo, Y.; Messinger, R. J.; Chmelka, B.; Ryoo, R. *Science* **2011**, *333*, 328. (f) Jiang, J.; Jorda, J. L.; Yu, J.; Baumes, L. A.; Mugnaioli, E.; Diaz-Cabanas, M. J.; Kolb, U.; Corma, A. *Science* **2011**, *333*, 1131. (g) Qin, Z.; Shen, B.; Gao, X.; Lin, F.; Wang, B.; Xu, C. *J. Catal.* **2011**, *278*, 266. (h) Zečević, J.; Gommes, C. J.; Friedrich, H.; de Jongh, P. E.; de Jong, K. P. *Angew. Chem., Int. Ed.* **2012**, *51*, 4213. (i) Liu, F.; Willhammar, T.; Wang, L.; Zhu, L.; Sun, Q.; Meng, X.; Carrillo-Cabrera, W.; Zou, X.; Xiao, F.-S. *J. Am. Chem. Soc.* **2012**, *134*, 4557.

(9) (a) Choi, M.; Na, K.; Kim, J.; Sakamoto, Y.; Terasaki, O.; Ryoo, R. *Nature* **2009**, *461*, 246. (b) Na, K.; Park, W.; Seo, Y.; Ryoo, R. *Chem. Mater.* **2011**, *23*, 1273. (c) Kim, J.; Park, W.; Ryoo, R. *ACS Catal.* **2011**, *1*, 337. (d) Chen, H.; Wydra, J.; Zhang, X.; Lee, P. S.; Wang, Z.; Fan, W.; Esapatsis, M. *J. Am. Chem. Soc.* **2011**, *133*, 12390. (e) Zhang, X.; Liu, D.; Xu, D.; Asahina, S.; Cychosz, K. A.; Agrawal, K. V.; Wahedi, Y. A.; Bhan, A.; Hashimi, S. A.; Terasaki, O.; Thommes, M.; Tsapatsis, M. *Science* **2012**, *336*, 1684. (f) Deng, Y.; Yin, S.; Au, C. *Ind. Eng. Chem. Res.* **2012**, *51*, 9492. (g) Inayat, A.; Knoke, I.; Spiecker, E.; Schwieger, W. *Angew. Chem., Int. Ed.* **2012**, *51*, 1962.

(10) Medici, L.; Prins, R. *J. Catal.* **1996**, *163*, 38.

(11) (a) Fierro, F. L. G.; Conesa, J. C.; Lopez-Agudo, A. *J. Catal.* **1987**, *108*, 334. (b) Li, D.; Xu, H.; Guthrie, G. D., Jr. *J. Catal.* **2000**, *189*, 281. (c) Leyrit, P.; Cseria, T.; Marchal, N.; Lynch, J.; Kasztelan, S. *Catal. Today* **2001**, *65*, 249.